

Proteins Immobilized at the Galleries of Layered α -Zirconium Phosphate: Structure and Activity Studies

Challa V. Kumar* and Anita Chaudhari

Contribution from the Department of Chemistry, U-60, University of Connecticut, 55 North Eagleville Road, Storrs, Connecticut 06269-4060

Received September 10, 1999

Abstract: Facile immobilization of myoglobin (Mb), lysozyme (Lys), hemoglobin (Hb), chymotrypsin (CT), and glucose oxidase (GO) at the interlayer regions of layered α -zirconium phosphate (α -ZrP) under ambient conditions (pH 7.2, room temperature) is described. The proteins retain their structure and activity after immobilization. The interlayer spacings of α -ZrP (observed in powder XRD experiments) increased from 7.6 Å (for α -ZrP) to 53, 47, 66, 62, and 108 Å when Mb, Lys, Hb, CT, and GO are bound to the matrix, respectively. These XRD data strongly suggest intercalation of the proteins in the galleries. The binding constants of the above proteins with α -ZrP, estimated from the centrifugation method, are in the range of 10^4 – 10^6 M⁻¹. The α , β , and the solet absorption bands of Mb/Hb immobilized on α -ZrP were essentially superimposable with those of the native proteins in solution. The FTIR spectra of the enzyme– α -ZrP composites, measured with an attenuated total reflectance accessory, show that the amide I and amide II bands of the immobilized proteins correlate well with those of the free proteins. The circular dichroism (CD) spectra of immobilized proteins, similarly, are quite similar to those of the corresponding native proteins. These various spectral investigations are consistent with high affinity binding of the proteins to α -ZrP with considerable retention of protein structure. Activities of the immobilized proteins are investigated for comparison with those of the proteins in solution. The hydrolytic activity of immobilized lysozyme is essentially the same as that of the free protein. CT and GO showed small but reproducible increases in their activities upon immobilization. The enzymatic activity parameters, K_m and V_{max} , observed for the immobilized Mb, lysozyme, and GO are comparable to those of the native proteins. The peroxidase activity of Mb/Hb depended on the substrate structure. Activities are higher for the immobilized Mb when *p*-methoxyphenol, phenol, and *m*-aminophenol are used as the substrates. The activities have been lower, on the other hand, when aniline, *o*-cresol, and *o*-aminophenol are used as the substrates. In general, the ratio of the specific activities of immobilized Mb to those of free Mb roughly increases with increased substrate oxidation potential. The interlayer spacings observed for the protein– α -ZrP composites show a strong correlation with the average size of the protein, and this method may be useful for the determination of protein size. The binding affinities of the proteins correlate with their respective pI values, with the exception of Hb, suggesting the role of electrostatic interactions in the binding process. The average area occupied per protein molecule is larger than the average area of cross section of the proteins, and the area occupied correlates with the reciprocal of the corresponding binding constants. These studies indicate that the hydrophilic character of the matrix and its surface charge are important attributes that influence the bound protein behavior. Enhanced activity of Mb with specific substrates and improved activities of CT and GO are additional advantages of immobilization. Control over the immobilized protein properties is important for their application in biosensors and biocatalysis.

Introduction

Enzymes are highly efficient and specific catalysts, but their routine use in chemical transformations is severely limited by their high cost and poor stability. Immobilization of enzymes at solid surfaces can partly overcome these limitations.¹ Immobilized enzymes can be recycled, thereby lowering their effective cost; the immobilized catalyst can easily be separated from the reaction mixture for easy workup; and reactions may be carried out in organic solvents. Immobilization can stabilize enzymes in specific cases, with improved activity, and in few

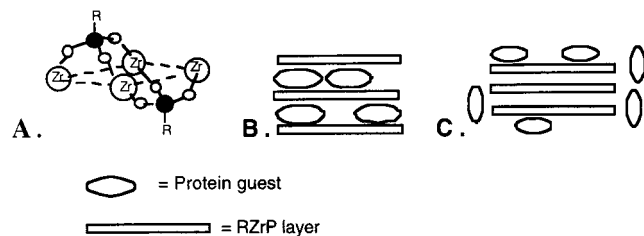
instances the selectivity of the enzyme is altered in a desirable way.² Although the interaction between the protein and the support matrix is expected to play a major role in attenuating the immobilized enzyme properties, the effect of surfaces on the immobilized proteins is not well-understood. Immobilization of proteins at well-defined surfaces and study of their properties is necessary for understanding immobilized protein behavior. Developing a general methodology for the immobilization of proteins at well-defined hydrophilic solid surfaces and correlating their properties with the support surface characteristics, therefore, has been our interest. Such studies may be useful in identifying specific surfaces that improve the properties of the immobilized enzymes and in understanding the enzyme–matrix

* Author to whom correspondence should be addressed.

(1) (a) Gubitz, G.; Kunnsberg, E.; van Zoonen, P.; Jansen, H.; Gooijer, C.; Velthorst, N. H.; Fei, R. W. *Chemically Modified Surfaces*; Leyden, D. E., Collins, W. T., Eds.; Gordon and Breach: London, 1988; Vol. 2, p 129. (b) Gorton, L.; Marko-Varga, G.; Dominguez, E.; Emneus, J. *Analytical Applications of Immobilized Enzyme Reactors*; Lam, S., Malikin, G., Eds.; Blackie Academic & Professional: New York, 1994; p 1.

(2) *Proteins at Interfaces II. Fundamental and Applications*; Horbett, T. A., Brash, J. L. Eds.; ACS Symposium Series 602; American Chemical Society: Washington DC, 1995.

Chart 1. Schematic representation of a single layer of α -zirconium phosphate (A). The R groups are oriented perpendicular to the plane of Zr(IV) (large circles), and six oxygens (small open circles) surround each Zr ion. Shaded circles are phosphorus atoms. In the case of α -ZrP, R is OH. Proteins may bind in the galleries of α -ZrP (B) and on the outer surfaces (C).



interactions. In addition to the above motivations, the importance of surface-bound proteins in biosensors, medical implants, enzyme reactors, and biomedical devices demands that a sufficient understanding of protein–surface interactions be developed such that the support matrix surfaces can be designed on a rational basis to maximize protein function.³

The support matrix, in general, should prevent enzyme aggregation, or spontaneous denaturation, and the matrix should not perturb the native properties of the immobilized protein to a significant extent in an undesirable way. The support matrix, in addition, should allow access to the immobilized enzymes by cofactors, substrates, or redox reagents.⁴ Enzymes have been immobilized, in this context, using polymers, sol gels, surfactant films, and hydrogels.⁵ The protective environment of these hosts can inhibit microbial degradation, hydrolysis, and deamidation, and can extend the useful lifetime of the bound proteins while preserving their activity.⁶ Binding of proteins at the surfaces of phospholipids,⁷ and Langmuir–Blodgett films have also been reported.⁸ These various studies clearly established the advantages of enzyme immobilization, although the support surface characteristics are not well-defined in many cases.

Layered α -zirconium phosphate ($\text{Zr}(\text{HPO}_4)_2 \cdot n\text{H}_2\text{O}$, abbreviated as α -ZrP, $R = \text{OH}$, Chart 1) is used as the support matrix in the current studies. α -ZrP is a well-characterized layered material with hydrophilic hydroxyl functions present on its two-dimensional lamellar surface (one OH per 24 \AA^2).⁹ Some advantages of using α -ZrP for protein immobilization are that the host has a layered structure and the α -ZrP layers can be readily expanded to accommodate small as well as large guest

molecules (from protons to proteins). α -ZrP is thermally stable and chemically inert in neutral/acidic media. The narrow galleries of α -ZrP may protect the bound proteins from microbial degradation. α -ZrP provides a large surface area upon exfoliation of the lamellae,¹⁰ and α -ZrP can present anionic surfaces (up to one negative charge per phosphate) for binding. α -ZrP binds metal ions, alkylammonium salts, metal complexes, organic cations, and proteins in the interlayer regions.¹¹ Immobilization of cytochrome c (cyt c) in the galleries of α -ZrP, for example, has been reported earlier.¹² Cyt c shows a high affinity for α -ZrP ($K_b > 10^6 \text{ M}^{-1}$), and upon binding to α -ZrP, Cyt c retained its spectroscopic features/redox activity. The hydrophilic nature of the α -ZrP surfaces (due to the OH groups) may play an important role in stabilizing the surface-bound protein. Acid phosphatase and amylase immobilized on hydrated tricalcium phosphate matrix, for example, retained their activities with increased thermal stability.⁸ The water molecules bound to the phosphate matrix are suggested to provide an aqueous-like medium to stabilize immobilized proteins.¹³ The surface hydroxyl functions of α -ZrP bind water and provide a suitable medium to immobilize hydrophilic proteins.

Binding of proteins to α -ZrP is expected to be dominated by electrostatic interactions. Positively charged proteins especially are expected to show high affinities for the anionic surfaces of α -ZrP (at pH 7.0). The excess surface charge on α -ZrP may not be favorable to some proteins, and in such cases the surface charge can be altered by adding appropriate electrolytes/buffer ions or by controlling the pH of the medium. Mild conditions required for ionic binding are expected to result in significant retention of enzyme structure and activity. Binding of penicillin G acylase to anionic methacrylate polymers, for example, increased immobilized enzyme stability when compared to the free enzyme.⁸ Ionic binding is labile, and this lability may be used as an advantage to remove the spent enzyme at high ionic strengths and to recharge the support matrix with the fresh enzyme.

Met-myoglobin (Mb), lysozyme (Lys), met-hemoglobin (Hb), glucose oxidase (GO), and α -chymotrypsin (CT) are chosen for the current studies.^{13–15} These proteins are well-characterized and provide several convenient attributes. Mb and Hb, for example, are heme proteins, and they have strong spectroscopic signatures that are suitable to monitor protein binding or their redox activity in the host environment.^{13,14} Hydrogen peroxide

(3) (a) *Biosensors in Analytical Biotechnology*; Freitag, R., Ed.; Academic Press: San Diego, 1996. (b) *Biosensor and Chemical Sensor Technology*; Rogers, K. R., Mulchandani, A., and Zhou, W., Eds.; ACS Symposium Series 613; American Chemical Society: Washington, DC, 1995.

(4) (a) Rosevear, A.; Kennedy, J. F.; Cabral, J. M. S. *Immobilized Enzymes and Cells*; Adam Hilger: Philadelphia, 1987.

(5) (a) Miksa, B.; Slomkowski, S. *Colloid Polym. Sci.* **1995**, *273*, 47. (b) Yoshinaga, K.; Kondo, K.; Kondo, A. *Polym. J.* **1995**, *27*, 98. (c) Tiberg, F.; Brink, C.; Hellsten, M. *Colloid Polym. Sci.* **1992**, *270*, 1188. (d) Yoishinaga, K.; Kito, T.; Yamaya, M. *J. Appl. Polym. Sci.* **1990**, *41*, 1443. (e) Shabat, D.; Grynspan, F.; Saphier, S.; Turniansky, A.; Avnir, D.; Keinan, E. *Chem. Mater.* **1997**, *9*, 2258.

(6) Fang, J.; Knobler, C. M. *Langmuir* **1996**, *12*, 1368. Mrksich, M.; Sigal, G. B.; Whitesides, G. M. *Langmuir* **1995**, *11*, 4383. Kennedy, J. F.; White, C. A. In *Handbook of Enzyme Biotechnology*; Wiseman, A., Ed.; Ellis Horwood Ltd.: Chichester, 1985, p147.

(7) (a) Kunitake, T.; Hamachi, I.; Fujita, A. *J. Am. Chem. Soc.* **1994**, *116*, 8811. (b) Fujita, A.; Senzu, H.; Hamachi, I. *Chem. Lett.* **1994**, 1219.

(8) Koilpillai, L.; Gradre, R. A.; Bhatnagar, S.; Raman, R. C.; Ponratham, S.; Kumar, K. K.; Ambekar, G. R.; Shewale, J. G. *J. Chem. Technol. Biotechnol.* **1990**, *49*, 173.

(9) (a) Clearfield, A.; Stynes, J. A. *J. Inorg. Nucl. Chem.* **1964**, *26*, 117. (b) Alberti, G.; Casciola, Costantino, U. *J. Colloid Interface Sci.* **1985**, *107*, 256.

(10) Upon exfoliation, the entire gallery surface can be exposed for binding, and each phosphate can provide up to 24 square angstroms of surface area. For example, the surface area available when butylamine is intercalated is estimated to be $100 \text{ m}^2/\text{g}$, and it is capable of exchanging 54 mM of cationic sites per gm (ecg); see Wan, B.-Z.; Anthony, R. G.; Peng, B. Z.; Clearfield, A. *J. Catal.* **1986**, *101*, 19.

(11) (a) Rosenthal, G. L.; Caruso, J. *J. Solid State Chem.* **1991**, *93*, 128. (b) Kumar, C. V.; Williams, Z. J. *J. Phys. Chem.* **1995**, *99*, 17632. (c) Clearfield, A.; Tindwa, R. M. *Inorg. Nucl. Chem.* **1979**, *41*, 871. (d) Clearfield, A. In *Inorganic Ion Exchange Materials*; Ed.; CRC: Boca Raton, FL, 1982. (e) Alberti, G. In *Recent Developments in Ion Exchange*; Williams, P. A.; Hudson, M. J., Eds.; Elsevier Applied Science: New York, 1987, 233. (f) Kumar, C. V.; Asuncion, E. H.; Rosenthal, G. L. *Microporous Mater.* **1993**, *1*, 123. (g) Kumar, C. V.; Asuncion, E. H.; Rosenthal, G. L. *Microporous Mater.* **1993**, *1*, 299. (h) Clearfield, A.; Constantino, U. In *Comprehensive Supramolecular Chemistry*; Atwood, J. L., Ed.; Pergamon: New York, 1996; Vol. 7, p 107.

(12) Kumar, C. V.; McLendon, G. L. *Chem. Mater.* **1997**, *9*, 863.

(13) (a) Das, G.; Prabhu, K. A. *Enzyme Microb. Technol.* **1990**, *12*, 625. (b) Monsan, P.; Combes, D. *Methods Enzymol.* **1988**, *137*, 584. (c) Kusano, S.; Shiraishi, T.; Takahashi, S.-I.; Fujimoto, D.; Sakano, Y. *J. Ferment. Biogeng.* **1989**, *68*, 233.

(14) Theorell, H. *Ark. Kemi Min. Geol.* **1942**, *15B*, 24. Dunford, H. B.; Adeniran, A. *J. Arch. Biochem. Biophys.* **1986**, *251*, 536. Job, D.; Dunford, H. B. *Eur. J. Biochem.* **1976**, *66*, 607. Sun, W.; Ji, X.; Kricka, L. J.; Dunford, H. B. *Can. J. Chem.* **1994**, *72*, 2159. Kelder, P. P.; de Mol, N. J.; Fischer, M. J. E.; Janssen, L. H. M. *Biochim. Biophys. Acta* **1994**, *1205*, 230.

reacts rapidly with Mb/Hb to generate the ferryl iron (Fe(IV)=O), which is capable of oxidizing amines, phenols, and other organic compounds. CT and lysozyme are hydrolytic enzymes with considerable potential for use in organic transformations, while GO is a redox enzyme widely used for blood-glucose monitoring.¹⁶

Immobilization of Mb, Hb, Lys, CT, and GO at the galleries of α -ZrP is reported here. Exposure of the exfoliated α -ZrP platelets to the above proteins leads to spontaneous binding of the proteins. Direct intercalation of proteins into the layered metal phosphates, without exfoliation of the layers, has also been reported, but these methods require extreme pH conditions (2–3 or >8) and long reaction times (as long as 17 days), and resulted in partial denaturation of the immobilized protein.¹⁷ Current results indicate that α -ZrP binds a variety of proteins (hydrolytic/redox) under mild conditions (neutral pH, and room temperature) with a significant retention of protein structure and activity. The resulting protein–inorganic composite matrices are examined by diffuse reflectance spectral methods (UV–Vis, FTIR, CD), powder X-ray diffraction (XRD), and activity studies. Such information on proteins immobilized at well-defined surfaces may be useful to learn how surface groups of the support matrix interact with proteins.

Experimental Section

Spectral Measurements. The absorption spectra were recorded on a Perkin-Elmer Lambda 3B spectrophotometer or HP 8453 diode array spectrometer using 1-cm cuvettes. α -ZrP suspensions of appropriate concentrations were used as reference samples to compensate for the light scatter by α -ZrP (<5% above 400 nm). Upon exfoliation with tetrabutylammonium hydroxide, the α -ZrP suspensions became translucent and scattered much less light.¹⁸

Protein Sources. Mb (horse skeletal muscle), Hb (bovine), GO (aspergillus niger type VII), lysozyme (chicken egg white), and α -chymotrypsin (bovine pancreas) are from Sigma Chemical Co. Protein solutions were made in potassium phosphate buffer (10 mM, pH 7.2) unless stated otherwise.

α -ZrP Synthesis. The metal phosphate was prepared according to published procedures, with minor modifications.⁹ Phosphoric acid (17 g, 172 mmol, 9 M) was added to ZrOCl₂ (10 g, 31 mmol). The reaction mixture was heated at 90 °C for 24 h. The resulting white product was washed twice with 50 mL of water and once with 20 mL of acetone. The solid was dried overnight at 60 °C. The FTIR spectra and the powder XRD pattern of the sample matched with those of the reported data.

Exfoliation and Immobilization of Proteins. Exfoliated α -ZrP (2%) suspensions were prepared by mixing 0.1 g of α -ZrP in 5 mL of distilled water with stoichiometric amounts of tetrabutylammonium hydroxide (40 wt % in water). The resulting suspensions were sonicated for 30–40 min and diluted with buffer as needed for the protein binding studies. Protein/ α -ZrP samples were prepared as reported earlier.¹² Stock solutions of the protein (0.5 mg/mL, 10 mM K₂HPO₄, pH 7.2) and exfoliated α -ZrP (2 wt %) are mixed in a 3:1 volume ratio. The mixture was equilibrated for 1 h and centrifuged to collect immobilized protein. In case of GO/ α -ZrP, the protein solution (2.3 mg/mL of GO, 10 mM potassium phosphate, 1 mM CaCl₂, pH 7.2) was mixed with exfoliated α -ZrP (2%) in a 3:1 volume ratio. Dry samples of the protein/ α -ZrP mixtures were prepared by lyophilizing the samples. The resulting solid was powdered for XRD or FTIR studies. For optical studies, the solid

was resuspended in phosphate buffer (0.01 wt % α -ZrP), and the protein/ α -ZrP suspensions scattered <5% of incident light above 400 nm.

Binding Stoichiometry Studies. Mb/ α -ZrP samples were prepared with increasing concentrations of Mb (10, 15, 20, 25, and 30 μ M). After equilibration for 1 h, the samples were centrifuged at 12 000 rpm in a Fisher Scientific minicentrifuge (Marathon 16KM), and the absorbance of the supernatant at 410 nm was recorded. Free protein concentration was plotted against the total protein concentration to estimate the stoichiometric coefficients. Lys/ α -ZrP samples contained increasing concentrations of Lys (6, 8, 12, 14, 17, and 21 μ M). After equilibration for 1 h, followed by centrifugation, the absorbance of lysozyme at 280 nm in the supernatant was monitored to construct the binding plots. Similarly, the binding stoichiometries of CT, Hb, and GO have been determined.

Binding Constant Measurements. The binding constants are estimated by the centrifugation method.¹² Mb/ α -ZrP samples contained 0.3 mM α -ZrP and varying concentrations of Mb (0.2, 0.4, 0.6, 0.8, and 1 μ M Mb, 12 mM potassium phosphate, pH 7.2). The samples were equilibrated for 1 h and then centrifuged at 12 000 rpm for 5 min to separate the free protein from the bound protein. Concentration of the free Mb in the supernatant was estimated from the absorbance of the samples at 410 nm. The binding data were plotted according to the Scatchard equation (eq 1).¹⁹

$$r/C_f = K_b (n - r) \quad (1)$$

In eq 1, r , C_f , K_b , and n are the binding density, the free protein concentration, the binding constant, and the binding site size, respectively. Binding density is the ratio of the concentration of the bound protein to that of the binding sites. A similar procedure was used to determine the binding constants of the other proteins.

XRD Studies. Protein/ α -ZrP suspensions (50–100 μ L) were spotted on glass slides and air-dried. XRD analysis of the immobilized protein samples was carried out with a Scintag Model 2000 diffractometer using nickel-filtered CuK α radiation. Scan rates for these runs were 2°/min. The interlayer separations were measured from the 00 l reflections ($l = 1, 2, \text{etc.}$) using Bragg's law.

FTIR Studies. A JASCO 410C spectrometer in the attenuated total reflectance (ATR) mode was used to record the protein/ α -ZrP FTIR spectra. Protein– α -ZrP suspensions were prepared in 10 mM K₂HPO₄ buffer (pH 7.2). After equilibration for 1 h, samples were centrifuged and the pellets were dried in vacuum for 3 h. ATR–FTIR spectra were recorded in the reflectance mode with 4 cm^{–1} resolution. Several scans (16–256) were averaged for each measurement, and the data have been replotted using KaleidaGraph (Version 3.0) software.

CD Studies. A JASCO model 710 spectropolarimeter was used to record the CD spectra from 190 to 300 nm. Scan rates were 50 nm/min with step resolution of 0.1 nm/data point. Bandwidth and sensitivity were 1 nm and 50 millidegrees, respectively. Several scans were accumulated for each sample, and the optical path length was 0.1 cm. CD spectra of the free proteins were recorded after placement of a suspension of α -ZrP in a separate cuvette in front of the sample cuvette to account for the attenuation of the CD signal due to light scatter by the particles. Use of α -ZrP, exfoliated α -ZrP, or butylamine intercalates of α -ZrP attenuated the signal to the same degree. Protein samples dissolved in 1 mL of buffer (10 mM K₂HPO₄, pH 7.2) were added to exfoliated α -ZrP (0.5%) as described earlier. After equilibration for 1 h, samples were centrifuged and pellets were resuspended in fresh buffer (10 mM potassium phosphate, pH 7.2). All protein/ α -ZrP suspensions were diluted as needed for the CD measurements.

Mb Activity Assay. The activity of Mb was followed using the reported procedure with minor modifications.²⁰ Stock solutions of Mb (103 μ M) and the substrate (*p*-methoxyphenol, 127 mM) were mixed with hydrogen peroxide in varying proportions. Substrate concentrations were increased from 0.5 to 4.0 mM (5 μ M Mb) while keeping the peroxide concentration constant (0.5 mM), and blank runs contained no peroxide (diluted with an equivalent volume of water). The product

(15) (a) Hecht, H. J.; Kalisz, H. M.; Hendle, J. *J. Mol. Biol.* **1993**, *229*, 153. (b) Zubay, G. In *Biochemistry*; Addison-Wesley: Boston, 1983.

(16) *Commercial Biosensors*; Ramsay, G., Ed.; J. Wiley and Sons: New York, 1998.

(17) (a) Ding, Y.; Jones, D. J.; Maireles-Torres, P.; Roziers, J. *Chem. Mater.* **1995**, *7*, 562. (b) Kanzaki, Y.; Abe, M. *Bull. Chem. Soc. Jpn.* **1991**, *64*, 2292.

(18) Mallouk, T. E.; Keller, S. W.; Kim, H.-N. *J. Am. Chem. Soc.* **1994**, *116*, 8817. Cao, G.; Hong, H.-G.; Mallouk, T. E. *Acc. Chem. Res.* **1992**, *25*, 420.

(19) Marshall, A. G. In *Biophysical Chemistry, Principles, Techniques, and Applications*; Wiley & Sons: New York, 1978; p 70.

(20) Maehly, A. C.; Chance, B. *Methods Biochem. Anal.* **1954**, *1*, 357.

formation was monitored as a function of time using a diode-array spectrophotometer in the kinetics mode. Sample spectra were recorded for 20–30 min while monitoring the absorbance at 470 nm every 10 s. Mb/ α -ZrP samples contained 5 μ M Mb, 1 mM α -ZrP with varying concentrations of the substrate, and 0.5 mM hydrogen peroxide. Lineweaver–Burke plots were constructed using these data, and K_m as well as V_{max} values have been calculated from these plots using eq 2.¹⁹ K_m is the Michaelis constant (substrate concentration when the rate is half of V_{max}), V_{max} is the maximum reaction velocity, and $[S]$ is the substrate concentration.

$$1/V = K_m/(V_{max} [S]) + 1/V_{max} \quad (2)$$

Lysozyme Activity Assay. Lysozyme activity was monitored using the reported procedure with some modifications.²¹ Lysozyme (60 μ M) and various concentrations of the substrate (glycol chitin, 0.05% to 0.30 wt %) were incubated at 40 °C for 1.25 h. To these solutions (1.5 mL each) were added 2 mL of 1.5-mM potassium ferricyanide (in 0.5 M sodium carbonate). Samples were then heated in boiling water for 30 min and cooled to room temperature, and the product absorption at 420 nm was observed. A standard calibration curve of absorption vs product concentration was constructed by mixing stock solutions of ferricyanide and n-acetylglucosamine. Lys activity was estimated by using this standard curve, and the activity of immobilized enzyme (7 μ M Lys, 1.5 mM α -ZrP, 12 mM phosphate, pH 7.2) was determined in a similar way.

CT Activity Assay. Activities of free and immobilized chymotrypsin were measured following a reported procedure with minor modifications.²² Protein solutions (114 μ M) were prepared in 20 mM tris buffer (38 mM CaCl_2 , 25% methanol, pH 7.8). The CT/ α -ZrP sample was resuspended in the above tris buffer. Protein samples (1 μ M) were mixed with *N*-benzoyl-L-tyrosine ethyl ester (BTEE). Absorbance at 254 nm was recorded after 1, 12, and 24 h after the start of the reaction. Rates were calculated based on the differences in the absorbances of the product and the starting material, using reported extinction coefficients.²²

GO Activity Assay. Activities of the free and immobilized glucose oxidase were measured following a reported procedure with some modifications.²³ Pyrenyl-1-butyrate (1 μ M) was added to the protein solution (0.6 μ M glucose oxidase, 1 mM CaCl_2), and the reaction was initiated by the addition of glucose (2 mM). The increase in the fluorescence intensity at 375 nm (excitation at 340 nm) was monitored as a function of time. For the immobilized glucose oxidase assay, the α -ZrP bound enzyme was resuspended in phosphate buffer (10 mM phosphate, pH 7.2, 0.6 μ M GO, 0.1 mM CaCl_2). The fluorescence growth curves were fitted using KaleidaGraph software (version 3.0), and the first-order rate constants were extracted from the data. The initial reaction velocities were used to construct Lineweaver–Burke plots, and the catalytic parameters were calculated from these plots.

Results

A general procedure for the intercalation of proteins into the galleries of α -ZrP under mild ambient conditions (pH 7, room temperature) is described here. Immobilized proteins are active, and they show high affinities ($K_b \approx 1 \mu\text{M}^{-1}$) for the α -ZrP matrix. A mild environment is indicated from the spectral data and activity studies. In specific cases, the immobilized proteins show improved activities.

Binding Studies. When equilibrium mixtures of α -ZrP/protein suspensions (1.5 mM α -ZrP, 12 mM K_2HPO_4 , pH 7.2, 0–13 μ M of protein) are centrifuged, the α -ZrP bound protein settles to the bottom and separates from the free protein. The free protein concentrations in the supernatant have been determined, and the corresponding binding stoichiometry plots are shown in Figure 1 a–d. Free protein concentration (C_f) was

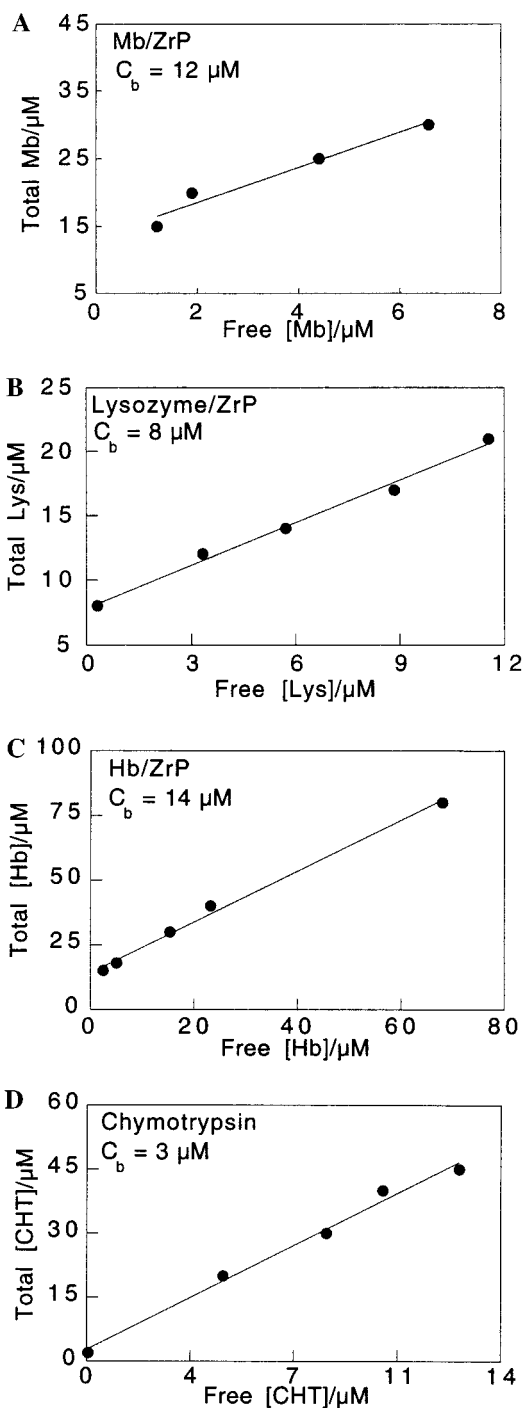


Figure 1. Stoichiometry plots for Mb, Lys, Hb, and CT (a through d, respectively). The concentration of α -ZrP (5 mM potassium phosphate, pH 7.2) was kept constant at 1.5 mM for all proteins, except that 0.3 mM α -ZrP was used for lysozyme.

smaller than total protein concentration (C_t) at all the protein concentrations examined, confirming the binding of the protein to α -ZrP. From the y intercepts of these binding plots, the binding stoichiometries have been estimated ($C_t = C_b + C_f$). The C_b values (1.5 mM α -ZrP) estimated for Mb, Lys, Hb, CT, and GO are 12, 40, 14, 3, and 1.1 μM , respectively (Table 1). These studies clearly establish the binding of the above proteins to the α -ZrP matrix.

Binding Constants. Equilibrium mixtures of α -ZrP with increasing concentrations of the protein were centrifuged, and we estimated the concentrations of the bound protein. These binding data are analyzed using the Scatchard equation (eq 1),¹⁹

(21) Imoto, T.; Yagishita, *Agric. Biol. Chem.* **1971**, *35*, 1154.

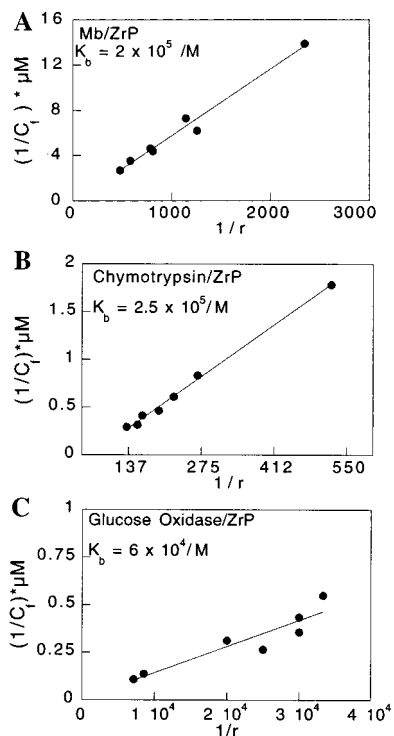
(22) Hummel, B. *Canadian J. Biochem. Physiol.* **1959**, *37*, 1393.

(23) Sierra, J.; Galban, J.; Castillo, J. R. Determination of Glucose in Blood Based on the Intrinsic Fluorescence of Glucose Oxidase. *Anal. Chem.* **1997**, *69*, 1471.

Table 1. Interlayer Spacings, Stoichiometries, and Binding Constants Observed for Immobilized Protein/ α -ZrP Composites^a

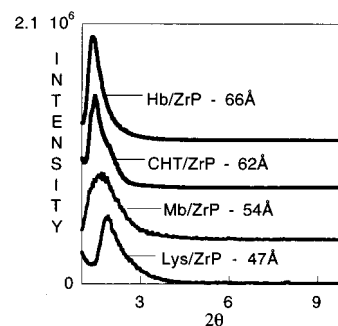
protein/ α -ZrP	stoichiometry (μ M)	K_b/M^{-1}	d spacing (\AA)	protein size (\AA)
no protein			7.6	
tetrabutylammonium			18.6	
myoglobin	12	2×10^5	54	$30 \times 40 \times 40$ (37)
lysozyme	40	1.33×10^6	47	$32 \times 32 \times 55$ (40)
hemoglobin	14	5.4×10^6	66	$53 \times 54 \times 65$ (57)
chymotrypsin	3	2.5×10^5	62	$40 \times 43 \times 65$ (49)
glucose oxidase	1.1	5.6×10^4	116	$43 \times 51 \times 68$ (54)

^a Protein dimensions are estimates from the known crystal structures and the average of the three dimensions is given in parentheses.

**Figure 2.** Scatchard plots for the binding of Mb, CT, and GO to α -ZrP (a through c, respectively).

and the binding plot for Mb is shown in Figure 2a. The binding constant for Mb calculated from this plot is $2 \times 10^5 \text{ M}^{-1}$, comparable to that of horseradish peroxidase.¹² In the cases of lysozyme and Hb, the binding constants are higher, 1.3×10^6 and $5.5 \times 10^6 \text{ M}^{-1}$, respectively (Table 1). Similarly, the binding constants for GO and CT are 5.6×10^4 and 2.5×10^5 (Figure 2b,c), respectively. These protein affinities for α -ZrP clearly demonstrate the ability of the metal phosphate matrix to bind a variety of water-soluble proteins with reasonable affinities. The binding of the proteins in the interlayer regions of α -ZrP was tested in powder X-ray diffraction experiments.

Intercalation into α -ZrP Galleries and Expanded Inter-layer Spacings. The XRD patterns of α -ZrP/protein complexes are presented in Figure 3. Immobilization of Mb, Lys, Hb, CT, and GO in the galleries of the α -ZrP matrix is indicated by the expanded interlayer spacings indicated by the powder diffraction patterns. The d spacings increased from 7.6 \AA for α -ZrP to 53, 47, 66, 62, and 108 \AA for samples containing Mb, Lys, Hb, CT, and GO, respectively. The peaks corresponding to α -ZrP (7.6 and 3.8 \AA , for example) and that of the tetrabutylammonium intercalated α -ZrP (17 \AA) are absent in the XRD patterns of the protein α -ZrP intercalates. New peaks, thus, appeared at lower 2θ values that indicate increased d spacings (Table 1). Larger proteins showed higher spacings, and the observed interlayer distances correlate with the respective sizes of the proteins.²⁴

**Figure 3.** Powder X-ray diffraction patterns of protein/ α -ZrP composite materials. The interlayer distance after protein binding is indicated.

The XRD peaks are sharp given the large protein dimensions, and the broad peak observed for Mb may indicate a distribution of orientations, whereas in other cases the distribution is narrow. Such a distribution may be important for the substrates to access the active sites of the bound proteins, unless the orientation exposes the active site. The observed d spacings with Mb, Lys, Hb, and CT are slightly larger than that of a monolayer of proteins at the galleries (Table 1), and a bilayer packing of the proteins at the galleries will require d spacings much larger than the observed values. Perhaps these proteins carry counterions, co-ions, and water molecules into the galleries, expanding the layers by slightly more than a monolayer thickness. In the case of GO, however, a bilayer packing appears to be involved with a d spacing of 108 \AA , twice its average size ($2 \times 54 \text{ \AA}$). The XRD data, therefore, provide strong evidence for the intercalation of proteins into the galleries of α -ZrP. The bound protein characteristics are examined in FTIR, CD, and activity studies.

Infrared Spectra. Immobilization of proteins at solid surfaces, in some cases, results in the loss of native conformation to a significant extent or denaturation. Such structural changes can be followed by monitoring the infrared absorption and circular dichroism spectra of proteins.^{25,26} The amide vibrational frequencies of proteins, for example, are sensitive to hydrogen bonding interactions of the amide function with the solvent, and with the neighboring functionalities. Protein denaturation modifies these interactions to a significant extent, and the amide vibrational frequencies shift. Accordingly, the amide I (assigned to the stretching of the carbonyl coupled to the C–N) and amide II vibrational bands are used as sensitive markers of protein

(24) (a) Kendrew, J.; Phillips, D.; Stone, V. *Nature* **1960**, *184*, 422. (b) Dickerson, R.; Kopka, M.; Weinzierl, J.; Warun, J.; Eisenberg, D.; Margoliash, E. *J. Biol. Chem.* **1967**, *242*, 3015. (c) Perutz, M.; Muirhead, H.; Cox, J.; Goaman, L.; Mathews, L.; McGandy, E.; Webb, L. *Nature* **1968**, *219*, 29. Sizes were estimated using data from the protein data bank and using Chem3D Pro.

(25) Torii, H.; Tasumi, M. In *Infrared Spectroscopy of Biomolecules*; Mantsch, H. H., Chapman, D., Eds.; John Wiley & Sons: New York, 1996; pp 1–18. Krimm, S.; Bandekar, J. *Adv. Protein Chem.* **1986**, *38*, 181. Susi, H.; Byler, D. M. *Methods Enzymol.* **1986**, *130*, 290. Pancoska, P.; Wang, L.; Keiderling, T. A. *Protein Sci.* **1993**, *2*, 411.

(26) Woody, R. W. In *Circular Dichroism and Conformational Analysis of Biomolecules*; Fasman, G. D., Ed.; Plenum Press: New York, 1996; pp 25–27. Gratzer, W. B.; Cowburn, D. A. *Nature* **1969**, *222*, 426.

Table 2. Relative Rates for the Oxidation of Various Substrates with Mb/H₂O₂ (bound to α -ZrP vs Free)^a

protein	amide I/amide II band (cm ⁻¹)	CD peaks (nm)	specific activity	K _m	V _{max}
Mb	1651/1530	210/222	3.3 × 10 ⁻³ /s	1.4 mM	0.08 μM/s
Mb/ α -ZrP	1651/1530	210/222	2.0 × 10 ⁻³ /s	1.6 mM	0.04 μM/s
Lys	1650/1521	207/223	11 × 10 ⁻³ /s	0.5 mM	0.63 μM/s
Lys/ α -ZrP	1650/1521	207/223	9.4 × 10 ⁻³ /s	0.5 mM	0.63 μM/s
Hb	1653/1521	210/222	0.013/s	0.103 mM	34 nM/s
Hb/ α -ZrP	1653/1521	210/222	0.038/s	0.112 mM	42 nM/s
CT	1656/1523	202/231	312/Ms		
CT/ α -ZrP	1658/1523	202/231	400/Ms		
GO	1645/1538	210/218	2 × 10 ⁵ /Ms	0.8 mM	0.037mM/s
GO/ α -ZrP	1645/1538	210/218	2.5 × 10 ⁵ /Ms	2.5 mM	0.042mM/s

^a Substrate concentrations were the same in all cases (6.6 mM), while Mb concentration was (5 μM).

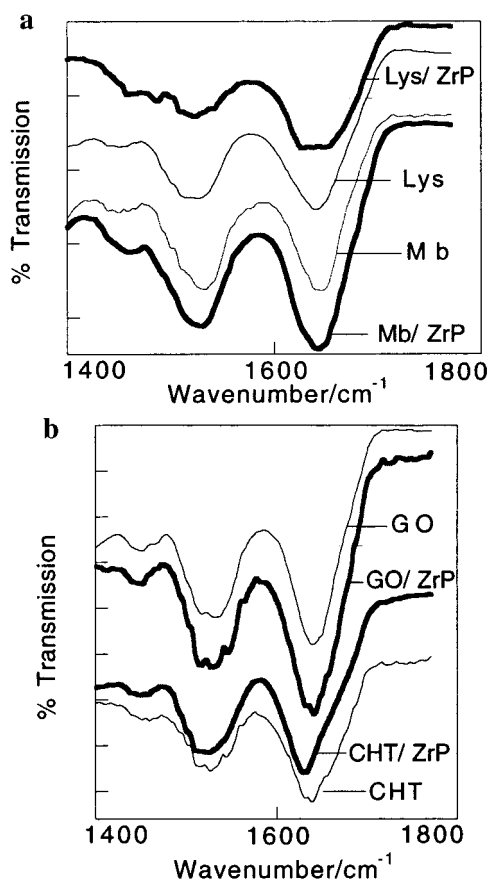


Figure 4. FTIR spectra of free and immobilized proteins recorded using the ATR accessory. Parts a, b correspond to the spectra of Mb, Lys, and CT, GO, respectively.

structural changes. Upon denaturation of an α -helix, for example, the amide I band shifts from 1650 cm⁻¹ to 1640 cm⁻¹, while the amide II band shifts to higher frequencies from 1550 cm⁻¹. The FTIR spectra of Mb, Lys, Hb, CT, and GO bound to α -ZrP, as well as the corresponding native protein spectra, are recorded (Figure 4a,b). The amide I and II vibrational bands of the bound Mb, Lys (Figure 4a), for example, are nearly superimposable with those of the free protein (Table 2). The amide bands of Hb and GO, similarly, did not change after immobilization on α -ZrP (Figure 4b). A small shift in the amide I band of CT is evident, indicating the sensitivity of CT to its microenvironment, rather than denaturation. The FTIR data indicate no major structural changes when the proteins are bound to the matrix.

Circular Dichroism Studies. The chiral nature of the protein building blocks and their arrangement in the secondary structure result in characteristic circular dichroism (CD) spectra. Double

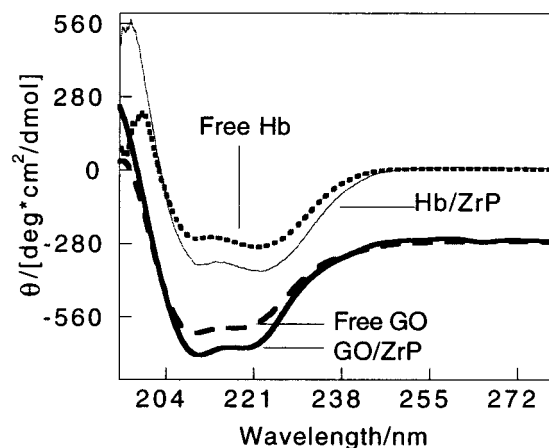


Figure 5. The circular dichroism spectra of Hb and GO, free and bound to the α -ZrP matrix, as indicated. The vertical axes of GO and GO/ZrP were offset by 400 ellipticity values. The peak positions of the free protein match with those of the bound protein.

minima at 210 and 222 nm are characteristic of α -helices, whereas the β -sheets exhibit a single, broad, negative peak at 212 nm, and random coils show a strong, sharp, negative peak at 195 nm.²⁶ The CD spectra of the immobilized proteins should indicate whether immobilization induces denaturation or unwinding of the protein structure. The CD spectra of the immobilized Mb, Lys, Hb, CT, and GO are nearly superimposable with those of the native proteins, and the CD spectra of Hb and GO, as representative examples, are shown in Figure 5. The CD peak positions of Mb, Lys, CT, and GO are summarized in Table 2. Little or no structural change is evident after immobilization of these proteins at the α -ZrP galleries. The CD spectra of immobilized proteins at other matrixes are not readily available for comparison. Loss of secondary structure, at any rate, can be readily identified from the CD spectra. Further insight into the behavior of the immobilized proteins was obtained from activity measurements. The access of the protein active site to the substrates, and the ease of diffusion of the reagents in to and out of the α -ZrP galleries, are examined in activity studies.

Activities of the Bound Proteins. Immobilized enzymes should retain their activity and be readily accessible for substrates.¹⁻⁹ The peroxidase activity of Mb/Hb, hydrolytic activity of Lys/CT, and oxidase activity of GO have been followed before and after immobilization. Oxidation of 4-methoxyphenol by Mb, in the presence of hydrogen peroxide, produces a colored tetrameric product, and this product provides a convenient spectrophotometric handle to monitor the peroxidase activity of Mb.²⁰ Oxidation of 4-methoxyphenol by the free and immobilized Mb (absorption monitored at 470 nm) is shown in Figure 6. Similarly, oxidation of glucose by GO, with

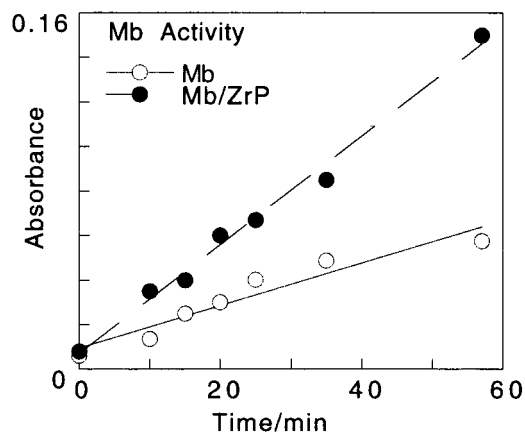


Figure 6. Peroxidase activity of free and immobilized Mb with *p*-methoxyphenol as the substrate.

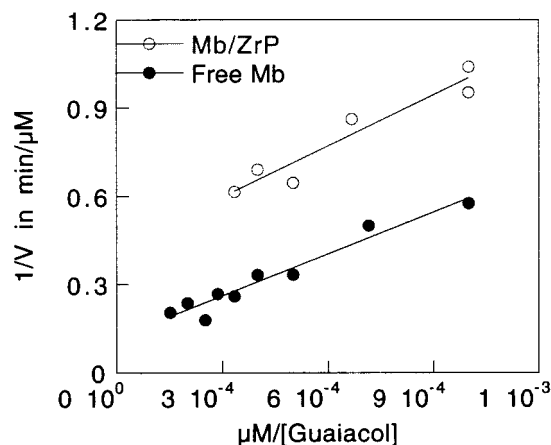


Figure 7. Lineweaver–Burke plot for the peroxidase activity of free and immobilized Mb with guaiacol as the substrate.

the concomitant consumption of oxygen, was monitored.²³ 4-(1-Pyrene)butyric acid (PBA) served as a convenient fluorophore to monitor oxygen concentration. The fluorescence from PBA is monitored as a function of time after the addition of glucose (2 mM) to a solution of GO (0.6 μM). The first-order growth curve of the fluorescence intensity was nearly the same for the immobilized and the free GO samples (Supporting Information 1). These results demonstrate the facile diffusion of the reactants and products through the layered support and the facile access to the active sites of the immobilized proteins. Encouraged by these results, we compared the K_m and V_{\max} values of the immobilized proteins with those of the free proteins.

The initial rates of product formation are recorded at different substrate concentrations, and these data were used to construct Lineweaver–Burke plots (Figure 7, Supporting Information 2a,b) to estimate K_m and V_{\max} values (using eq 2).¹⁹ The K_m for the bound Mb (5 μM), with guaiacol as the substrate, was 1.6 mM, larger than that of the free Mb (1.4 mM), whereas the V_{\max} for the bound protein was 2.5 $\mu\text{M}/\text{min}$, nearly half that of the free Mb (5.1 $\mu\text{M}/\text{min}$). The turnover numbers ($V_{\max}/[\text{enzyme}]$), therefore, for the bound and free Mb are 0.5 and 1.0 per min, respectively.

Lysozyme activity, similarly, was monitored by following the hydrolysis of glycol chitin, a known substrate for lysozyme. The initial velocities of the product formation are followed as a function of glycol chitin concentration, and the corresponding Lineweaver–Burke plots are linear (Supporting Information 2a). The rates of product formation for the bound protein are nearly the same as those of the immobilized protein ($K_m = 0.5$

monomer/ml, $V_{\max} = 38 \mu\text{M}/\text{min}$), suggesting that immobilization has little or no influence on lysozyme activity.

A Lineweaver–Burke plot for the immobilized GO is shown in Supporting Information 2b, and the corresponding catalytic parameters are collected in Table 2. The activities of the bound proteins are comparable to those of the free proteins, and in specific cases, the immobilized proteins showed better activities.

Discussion

Protein immobilization at well-defined solid surfaces is both challenging and interesting for applications in biosensors and biocatalysis. The experiments described here indicate successful immobilization of proteins at the anionic surfaces of α -ZrP, and the immobilized proteins retain their structure/activity. In specific cases, the enzyme activities are improved by immobilization.

The binding stoichiometries estimated for Mb, Lys, Hb, CT, and GO are 125, 38, 100, 500, and 2700 ZrP units, respectively. As each phosphate provides 24 \AA^2 of area at the galleries,^{11d} the number of phosphate groups occupied by the protein is expected to increase with the size of the protein. The radii of the average areas occupied by these proteins are 31, 17, 27, 61, and 143 \AA , respectively. However, these radii do not correlate well with the hydrodynamic radii of the proteins (19, 15, 48, 29, and 70 \AA , respectively).^{27–31} This is not surprising, because the average area occupied by the protein, under equilibrium conditions, also depends on the dissociation constant of the protein– α -ZrP complex. Weak binding (of GO, $K_b = 5.6 \times 10^4 \text{ M}^{-1}$) resulted in larger occupied area per protein (2700 ZrP units), whereas strong binding (of Lys, $K_b = 1.3 \times 10^4 \text{ M}^{-1}$) resulted in much less area occupied per molecule (38 ZrP units). Average area occupied by the protein (footprint) thus depends on the binding constants as well as their average sizes. Loose packing of the proteins, as in the case of GO, is perhaps important in maintaining access to the bound proteins by substrates and other reagents.

The binding constants observed for these proteins (Table 1) roughly correlate with the known pI values of the proteins,³² suggesting the strong role of electrostatic interactions in determining the binding constants. The moderate binding observed for Mb with α -ZrP ($2 \times 10^5 \text{ M}^{-1}$) is consistent with a pI of 7.0.¹⁷ The binding affinity of lysozyme (pI = 11.0),¹⁷ on the other hand, is much larger than Mb. In contrast, GO has the lowest affinity for α -ZrP, resulting from its low pI value (4.0).²⁰ Addition of MgCl_2 (1 M) to the protein/ α -ZrP composites suppresses binding (qualitatively), consistent with the role of electrostatic interactions in the binding process.

The interlayer distances measured for the protein/ α -ZrP composites provide strong evidence for protein intercalation in the galleries. The interlayer distances are larger than that of α -ZrP and tetrabutylammonium α -ZrP. The observed interlayer spacings, in addition, correlate with the average diameter of the proteins determined from the X-ray crystal data reported in the literature.³³ A plot of interlayer spacing vs average protein size is linear (Figure 8), and in the case of GO, twice the average

(27) Maire, M.; Rivas, E.; Moller, J. V. *Anal. Biochem.* **1980**, *106*, 12.

(28) Valstar, A.; Brown, W.; Mats, Al. *Langmuir* **1999**, *15* (7), 2366. Meredith, S. C.; Nathans, G. R. *Anal. Biochem.* **1982**, *121*, 234. Lysozyme is an ellipsoid with a minor axis of 14.6 \AA .

(29) Tarvers, R. C.; Church, F. C. *Int. J. Pept. Protein Res.* **1985**, *26*, 539.

(30) Schoenkecht, T.; Poerschke, D. *Biophys. Chem.* **1996**, *58*, 21.

(31) Burne, M.; Osicka, T.; Comper, W. *Kidney Int.* **1999**, *55*, 261.

(32) Marshall, A. G. In *Biophysical Chemistry, Principles, Techniques, and Applications*; Wiley & Sons: New York, 1978; p 70. Snell, E. E.; Di Mari, S. J. In *The Enzymes*, 3rd ed.; Boyer, P. D., Ed.; Academic Press: New York, 1970; Vol. II, pp 335–338.

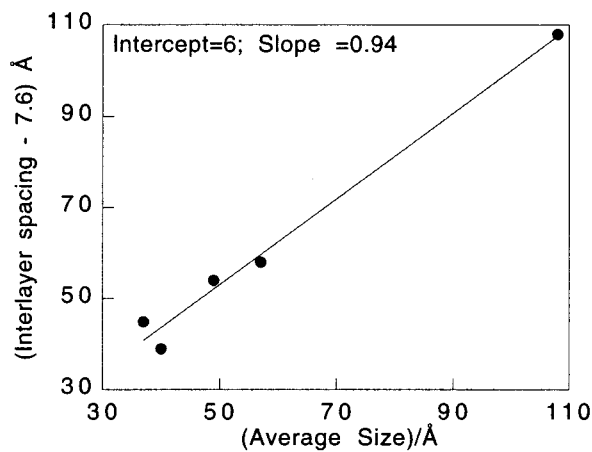


Figure 8. The observed interlayer spacings for the proteins/ α -ZrP composites correspond to the average sizes estimated from the crystallographic data.

protein size correlates with the observed spacing. This correlation is consistent with the bilayer packing of the enzyme at the galleries. The strong linear correlation found in the plot also reaffirms intercalation of the proteins in the galleries. The nonzero intercept (6 Å) in the plot is indicative of the average size of the hydration shell carried with the proteins into the interlayer regions, and this shell may contain co-ions and counterions as well.

The FTIR spectra of the immobilized proteins correlate well with those of the native proteins. The amide I and amide II peak positions estimated from the second derivative spectroscopy methods²⁵ (Table 2) indicate that the immobilized proteins experience a nativelike environment. These conclusions are bolstered by the CD spectra of the immobilized proteins. Taken together, FTIR and CD data clearly indicate that the structures of immobilized Mb, Lys, Hb, and GO have not been perturbed to any significant extent after immobilization. In case of CT, however, the amide I band is shifted from 1656 to 1659 cm^{-1} , and the amide II band is unchanged. But immobilization of CT did not perturb its CD spectrum, indicating that the changes in the IR spectra could be due to environmental effects rather than denaturation of the protein.

Activity studies of the immobilized proteins are encouraging. Large interlayer spacings observed for the immobilized materials (40–110 Å) should facilitate substrate access to the bound protein. The specific activities of Lys, CT, and GO are essentially the same as or slightly higher than those of the free proteins (Table 2). Some of the observed increases are within our error limits of $\pm 10\%$. The reason for the lower V_{max} value estimated for the immobilized Mb, as compared to that of the free Mb, is not due to protein denaturation or restricted access to the galleries. Immobilized Lys (with similar gallery spacing) is nearly as active as the free Lys, and the specific activities of CT and GO are slightly larger than those of the free enzymes. The reduction in V_{max} for the immobilized Mb could be due to the conformational restrictions imposed by the rigid matrix. Interestingly, the peroxidase activities of Mb and Hb are strongly modulated by the nature of the substrate.

In case of guaiacol, the product formation is slower with immobilized Mb when compared to that in buffer. 4-Methoxyphenol, in contrast, reacts more rapidly with the immobilized Mb than with free Mb (Figure 6). To evaluate the stereoelec-

Table 3. Ratio of the Rates of Peroxidase Activity of Immobilized Mb to Those of the Free Mb with Various Substrates^a

substrate	relative rate (bound/free)	oxidation potential/ V^{23}
<i>p</i> -methoxyphenol	2.54	0.406
<i>o</i> -methoxyphenol	0.24	0.456
phenol	1.26	1.04
<i>o</i> -cresol	0.31	0.556
aniline	0.97	0.70
<i>m</i> -aminophenol	1.75	
<i>o</i> -aminophenol	0.09	0.124

^a Oxidation potentials of the substrates are listed.

tronic factors effecting the oxidation by Mb, the rates of reactions with a number of substrates have been examined (Table 3). Rate accelerations are observed with phenol, *m*-aminophenol, and *p*-methoxyphenol. With all the *p*-isomers, the oxidation was accelerated by the immobilized Mb in comparison to that of the free protein, while the *o*-isomers reacted slower with the immobilized protein when compared to the free Mb. The *o*- and *p*-methoxy phenols (with similar oxidation potentials) showed large differences in the rate enhancements. One possibility is that the active site geometry of Mb/ZrP allows for better access to *p*-methoxy phenol while restricting access to the *o*-isomer, resulting in improved selectivity. The ratio of rates (rate with immobilized Mb to that with free Mb) correlates well with the substrate oxidation potential (Supporting Information 3), with the exception of *p*-methoxyphenol. In this small set of substrates, rate accelerations are associated with oxidation potentials greater than 0.7 V, while rate deceleration are observed below this potential. Binding of Mb to the negatively charged matrix alters Mb redox potential, and this can enhance or lower the observed rates. Changes in the oxidation potential of Mb bound to the negatively charged DNA helix were reported.³⁴ Enhanced activities and improved selectivities of immobilized enzymes, in specific cases, are additional benefits of immobilization, but such rate enhancements/improvements are rarely observed.^{2,3}

Conclusions

The spontaneous self-assembly of several proteins as single layers at the galleries of α -ZrP, at room temperature and pH 7.2, is demonstrated here. The binding constants correlate with the net charge of the proteins at pH 7.2. FTIR and CD spectra indicate no detectable changes in the immobilized protein structure. Immobilized proteins retain their activity, and in specific cases, small increases in the activities are observed. With Mb, substantial increases in the rates are observed with selected substrates. The activity studies clearly indicate the facile diffusion of small molecules or ions into and out of the galleries of protein- α -ZrP composites. Such access is necessary for the incorporation of these biocomposite materials in chemical or biological sensors. Similar studies with commercially important enzymes and specific host surfaces are underway.

Acknowledgment. The financial support for this work was provided by NSF (DMR-9729178) and the University of Connecticut Research Foundation. We are thankful to Professor S. L. Suib for access to the XRD equipment.

Supporting Information Available: Growth curve of fluorescence intensity for immobilized and free GO samples; Lineweaver–Burke plots estimating K_m and V_{max} values; plot of $K_{\text{bound}}/K_{\text{free}}$ vs oxidation potential (PDF). This material is available free of charge via the Internet at <http://pubs.acs.org>. JA993310U

(33) Takano, T. *J. Mol. Biol.* **1993**, *229*, 13. Imoto, T.; Johnson, L. N.; North, A.; Phillips, D. C.; Rupley, J. A. *The Enzymes*; Boyer, P. D., Ed.; Academic Press: New York, 1972; pp 665–808. Hecht, H. J.; Kalisz, H. M.; Hendle, J.; Schmid, R. D.; Schomburg, D. *J. Mol. Biol.* **1993**, *229*, 13.

(34) Nassar, A.-E. F.; Rusling, J. F.; Nakashima, N. *J. Am. Chem. Soc.* **1996**, *118*, 3043–4.